CHARACTERSIATION OF FIBRE-METAL-LAMINATES UNDER BEARING LOADING

B.Bosbach[1], H.Meeuw[1] and B.Fiedler[1]

[1]Institute of Polymer Composites, Technische Universität Hamburg,
Denickestraße 15, 21073 Hamburg
Email: bjoern.bosbach@tuhh.de, hauke.meeuw@tuhh.de, fiedler@tuhh.de,
Web Page: http://www.tuhh.de/kvweb

Keywords: Glass fibres, metals, Digital Image Correlation, Resin-Transfer-Moulding

Abstract
In this work fibre metal laminates (FML) consisting of glass fibre reinforced polymers (GFRP) with solid and permeable metal sheets are manufactured by vacuum assisted resin transfer moulding (VARTM). The results are composites of high quality without void imperfection. In the next step, the composites are investigated by quasi-static pin-loaded bearing tests. The bearing strain is measured by Digital Image Correlation (DIC).
The experimental bearing responses are compared whereas hybrids demonstrate a more ductile fracture behaviour and higher bearing strength in contrast to the conventional GFRP. The perforated metal sheet demonstrates a higher resistance against delamination compared to the solid metal sheet, which leads to a higher residual strength of this hybrid composite. Furthermore, it yields to a weight reduction compared to the solid metal sheet.

1. Introduction

One of the big challenges in the field of fibre reinforced polymers is to figure out a suitable way to introduce the mechanical load into the structure. In the aerospace industry and for rotor blades of wind turbines this is often realised by bolted joints. In general, the load capacity of a bolted joint is enhanced by locally increasing the laminate thickness and corresponding ply drop-off to the nominal thickness (Figure 1a).

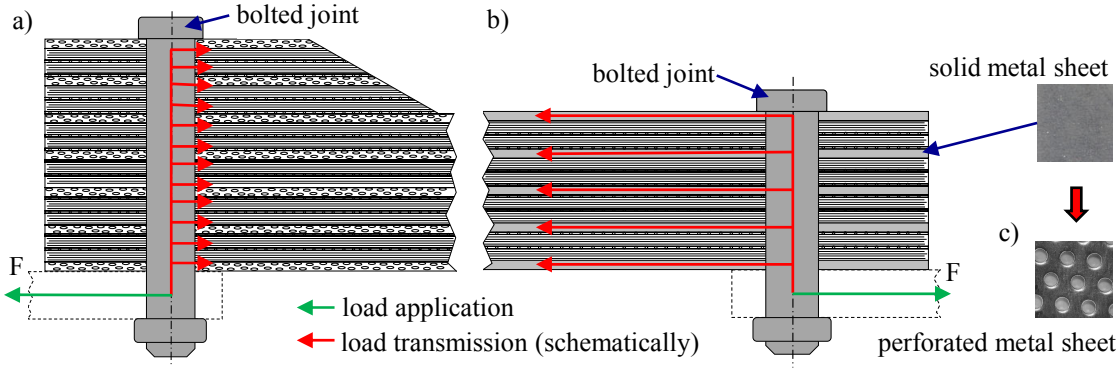

Figure 1. Load capacity of a bolted joint, a) FRP with increased laminate thickness, b) solid metal sheet and c) permeable metal sheet with constant laminate thickness.

Excerpt from ISBN 978-3-00-053387-7

However, this procedure increases the weight as well as causes secondary bending to the structure. An alternative to locally increase the laminate stress introducing capability is the replacement of single FRP layers with solid metal sheets (Figure 1b). These sheets allow a two-dimensional load introduction into the laminate. In the literature the influence on the compression/bearing loading of hybrid composites is deeply investigated. For increasing the load capacity and at the same time keeping the laminate thickness constant FML consisting of FRP and solid metal sheets were used. These hybrids are mostly manufactured by the prepreg-autoclave technology. The metal volume fraction of these laminates is mostly between 16-50 vol.-% metal [1–4]. Both et al. [5] compared the results of pure CFRP laminates with CFRP/titanium and CFRP/steel laminates by finite element analysis as well as experiments. The absolute bearing strengths increased significantly by substituting single CFRP-plies by thin metal sheets. However, the density specific values of pure CFRP were highest, followed by CFRP/titanium and CFRP/steel test results. Therefore a CFRP/metal laminate should only be considered if the thickness of the load introduction area must be of the similar thickness as the remaining part. Bosbach et al. [6] compared experimentally the bearing loading of FML consisting of GFRP and woven metallic fabrics (WMF) with a conventional GFRP laminate. The composites were manufactured by the VARTM. The absolute bearing strength increased by substituting single GFRP plies by WMF. The thickness of the load instruction area was similar to the remaining part. The ductility of the WMF yielded to an increased bearing strain and a good-natured failure.

In this work solid and perforated stainless steel sheets (Figure 1c) are used in a hybrid composite and compared with a conventional GFRP laminate. By using a permeable metal sheet the matrix can flow through all layers in thickness direction while the injection process, which increases the processing time. In addition, the permeable metal sheet yield to a weight reduction compared to the solid metal sheet. The pin-loaded bearing tests is conducted according to ASTM D-5961-Procedure A [7], with a self-made modified loading fixture, to enable observation of the specimen surface in front of the pin by DIC, according to [8]. The light microscopy (LM) is used to evaluate the fracture behaviour of the laminates after testing. The metal surface is not treated, to evaluate the influence of the permeability against delamination under bearing loading.

2. Material and Methods

2.1. Material

The quasi-isotropic GFRP composite consists of E-glass fibre (GF) non-crimp fabrics (NCF) (q_F=528g/m^2 in 0°-direction and q_F=54g/m^2 in 90°-direction) and biaxial (±45°) GF NCF (q_F=430g/m^2) (R&G Faserverbundwerkstoffe GmbH). For the hybrid composites the biaxial GF NCF are substituted by solid and perforated stainless steel sheets (JAERA GmbH & Co. KG). The material and volume fraction of a single layer are shown in Table 1. The metal sheets are cleaned with acetone before applying. A surface treatment is not conducted.

Table 1. Material, condition and volume fraction of a single ply.

Layer	Material	Condition	Volume fraction (%) of a single ply
$St_{77\%}$	X5CrNi18-10	perforated	77
$St_{100\%}$	X5CrNi18-10	solid	100

Excerpt from ISBN 978-3-00-053387-7

Figure 2 shows the structure and mass per unit area (q_F) of the used materials for the quasi-isotropic GFRP and hybrid composites.

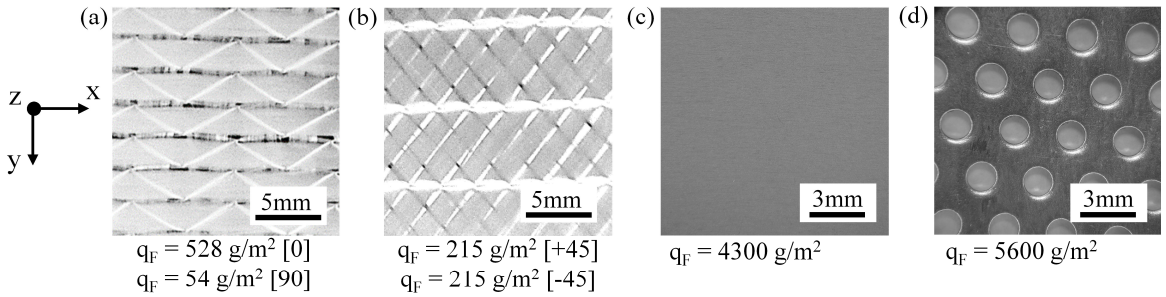

Figure 2. Structure and mass per unit area of the materials (q_F: mass per unit area): a) glass fibre NCF, b) biaxial glass fibre NCF c) solid stainless steel sheet, d) perforated stainless steel sheet.

Table 2 summarizes the lay-up and the mean value and standard deviation of the fibre volume fraction (V_f), metal volume fraction (V_{metal}), density (ρ) and onset glass transition temperature (T_G) of all laminates. T_G is measured by the differential scanning calorimetry (DSC) 204 F1 Phoenix® ASC (NETZSCH GmbH & Co).

Table 2. Lay-up and properties of the laminates.

Laminate	Lay-up	V_f(%)	V_{metal}(%)	ρ (g/cm³)	$T_{G,onset}$ (°C)
GFRP	$[\pm45_2,(0^{90\%},90^{10\%})_2,(90^{10\%},0^{90\%})]_s$	51,9±0,4	-	1,90±0,01	91,5±2,6
GFRP/$St_{100\%}$	$[St_{100\%},(0^{90\%},90^{10\%})_2,(90^{10\%},0^{90\%})]_s$	34,6±0,3	34,1±0,1	3,93±0,01	94,3±0,6
GFRP/$St_{77\%}$	$[St_{77\%},(0^{90\%},90^{10\%})_2,(90^{10\%},0^{90\%})]_s$	33,1±0,3	25,8±0,1	3,35±0,02	93,6±2,1

For the injection procedure the resin RIMR 135 and the hardener RIMH 137 (Momentive Inc.) are used [6]. During the VARTM-process the laminates are cured in a mould (t=4mm) at 60°C for 12 hours. After cutting and polishing the specimens are drilled (⌀6.3H7) by one-shot-drilling with a hard metal-drill and a circumferential speed of v_c=4000RPM. Afterwards all specimens are post cured at 80°C for 15 hours. To keep the specimens in constant condition the specimens are placed at least for 2 weeks in an exsiccator before testing allowing possible residual stresses to relax. All composites show a high inter- and intralaminar matrix wetting with no imperfections.

2.2. Experimental Methods

The pin-loaded bearing tests are conducted according to ASTM D-5961-Procedure A [7], with a self-made modified loading fixture (Figure 3), to enable observation of the specimen surface in front of the pin by DIC, according to [8]. The fixture assembly is made from stainless steel. The pin is made from 42CrMo4 steel (⌀6.3mm) and causes a transition fit between pin and hole. The edge distance to pin diameter (e/d) and width to pin diameter (w/d) are experimental pre-tested to cause bearing failure for all laminates. The final geometries are width (w) = 36mm and edge distance (e) = 26mm.

Excerpt from ISBN 978-3-00-053387-7

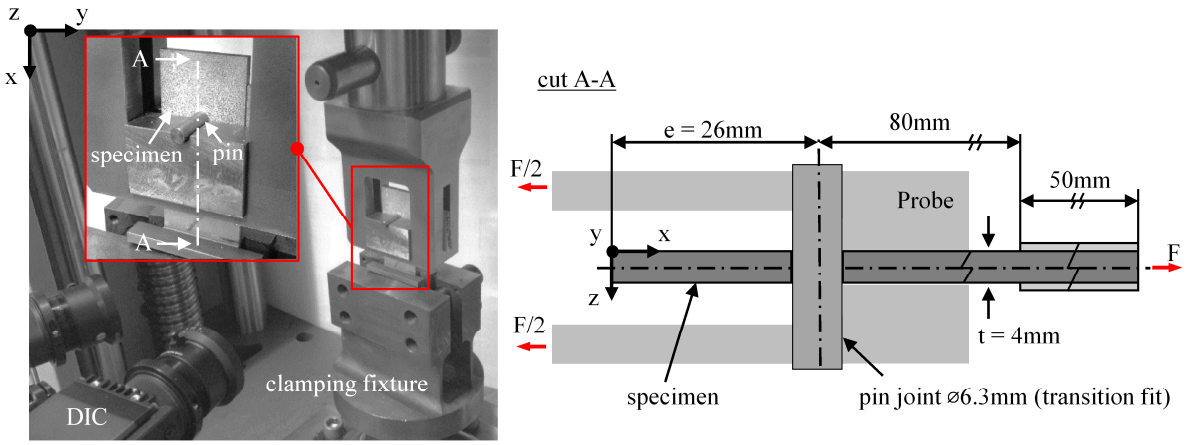

Figure 3. Loading fixture and geometries of the specimen according to ASTM D5961 [7].

The load-bearing test is performed in a universal tester Zwick BPC-F0400EN.R04. The head displacement rate is 2mm/min. The DIC system measures the bearing strain (ε_x) on the specimen surface. The load/displacement response is recorded.

3. Results and Discussion

Of each composite 3 specimens are tested and representative specimens are shown in the corresponding figures. The bearing stress (σ^{br})-bearing strain (ε^{br}) response, of all laminates is illustrated in Figure 4. All specimens fail by bearing. The hybrids demonstrate a higher bearing strength ($\sigma_{2\%}$) (2% hole expansion), ultimate bearing strength (σ_{ult}), bearing strain (ε^{br}) to failure and Young´s Modulus (E^{br}) compared to the conventional GFRP laminate. The distribution of the surface strain of the specimens, using three-dimensional DIC, is illustrated at approx. (σ^{br}~380MPa) and at the end of the load-bearing tests (Figure 4).

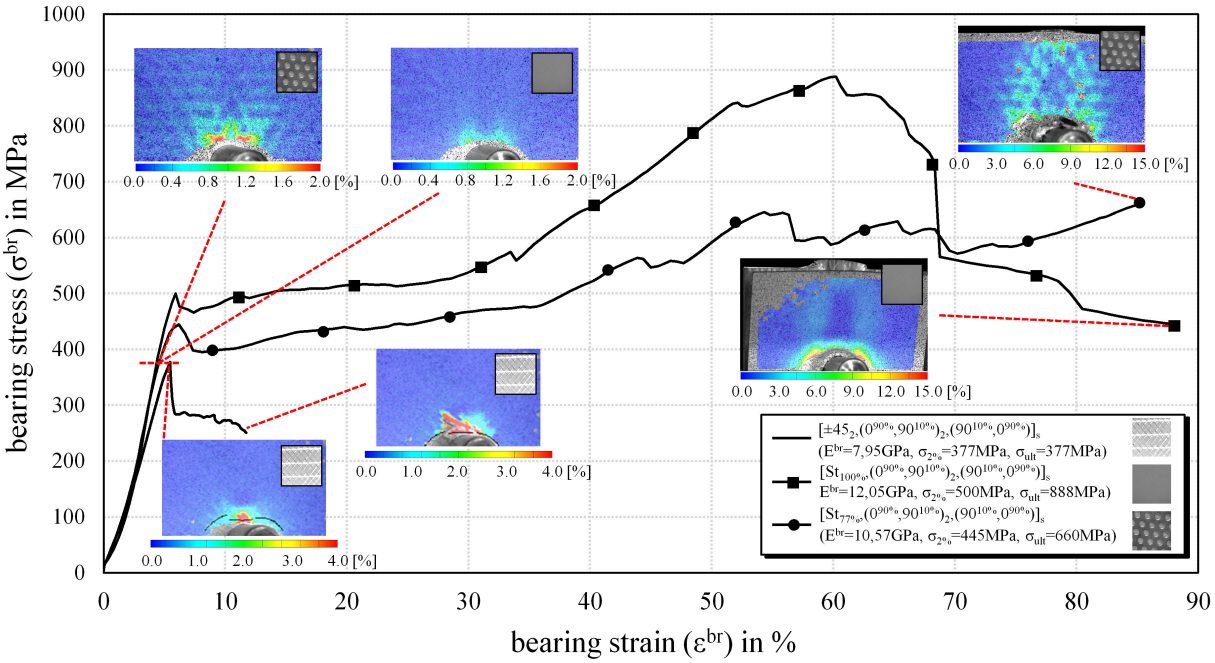

Figure 4. Bearing stress (σ^{br})-bearing strain (ε^{br}) response of all laminates.

Excerpt from ISBN 978-3-00-053387-7

At a bearing stress of σ^{br}~380MPa the hybrids yield to a significant lower surface strain in comparison to the GFRP (Figure 4, DIC). This is caused by the higher stiffness of the metal sheets compared to the biaxial GFRP layers. Table 3 summarizes the bearing strength ($\sigma_{2\%}$), ultimate bearing strength (σ_{ult}) of the laminates and the improvement of the hybrids compared to the GFRP.

Table 3. Bearing strength and ultimate bearing strength of the laminates.

Laminate	Bearing ($\sigma_{2\%}$) [MPa]	Improvement [%]	Ultimate bearing strength (σ_{ult}) [MPa]	Improvement [%]
GFRP	376±6	-	376±6	-
GFRP/$St_{100\%}$	501±7	33	887±13	136
GFRP/$St_{77\%}$	443±9	15	659±8	75

The following figures show the failure behaviour of representative laminates by LM micrographs of the cross section. The glass fibres are light grey, the resin dark grey, the metal sheets appear white. The GFRP specimen, shortly after 2% hole expansion ($\sigma_{2\%}$~370MPa), in Figure 5 shows fibre failures and kink-bands in the 0°-GF layers as well as interfibre-failure in the ±45°-GF layers. Further loading of a similar specimen demonstrates that these failure modes increase and the bearing stress drop down approx. 30% of the ultimate bearing strength.

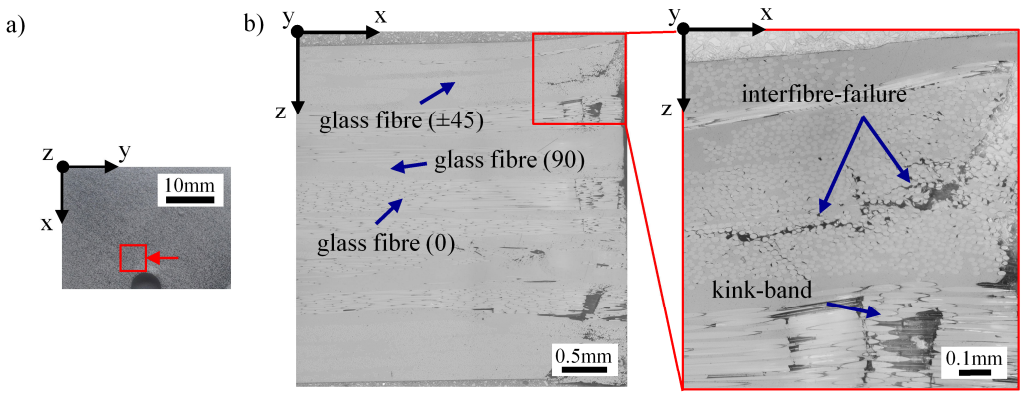

Figure 5. GFRP specimen shortly after 2% hole expansion ($\sigma_{2\%}$~370MPa)
a) sampling of the micrograph specimen, b) optical light microscopy.

Figure 6 shows a GFRP/$St_{100\%}$ specimen ($\sigma_{2\%}$~495MPa). At this point of loading a delamination between the untreated solid stainless steel sheets and the 0°-GFRP layers occurs. The 0°-GF layer shows a kink-band and the 90°-layers interfibre-failure. By observing a similar specimen after further loading the previous failure modes increase and the solid metal sheets completely delaminate. This causes the significant load drop at a bearing strain of ε^{br}~60% (Figure 4).

Excerpt from ISBN 978-3-00-053387-7

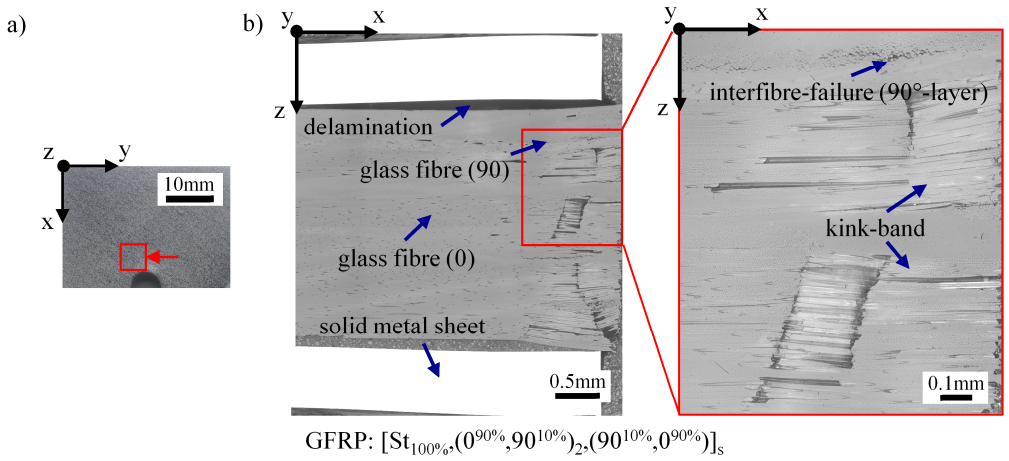

Figure 6. GFRP specimen shortly after 2% hole expansion ($\sigma_{2\%}$~495MPa)
a) sampling of the micrograph specimen, b) optical light microscopy.

Figure 7 shows a GFRP/$St_{77\%}$ specimen ($\sigma_{2\%}$~455MPa). This hybrid demonstrates similar failure modes as the previous GFRP/$St_{100\%}$. The kink-bands are more distinct in all 0°-GF layers in comparison to the hybrid GFRP/$Al_{100\%}$. By further loading a similar specimen the previous failure modes increase. Due to the permeability of the perforated metal sheets, the delamination initially stops by reaching a resin rich zone. Consequently, it prevents further delamination and buckling of the 0°-GF layers. After reaching a bearing strain of ε^{br}~85% the load still increases (Figure 4).

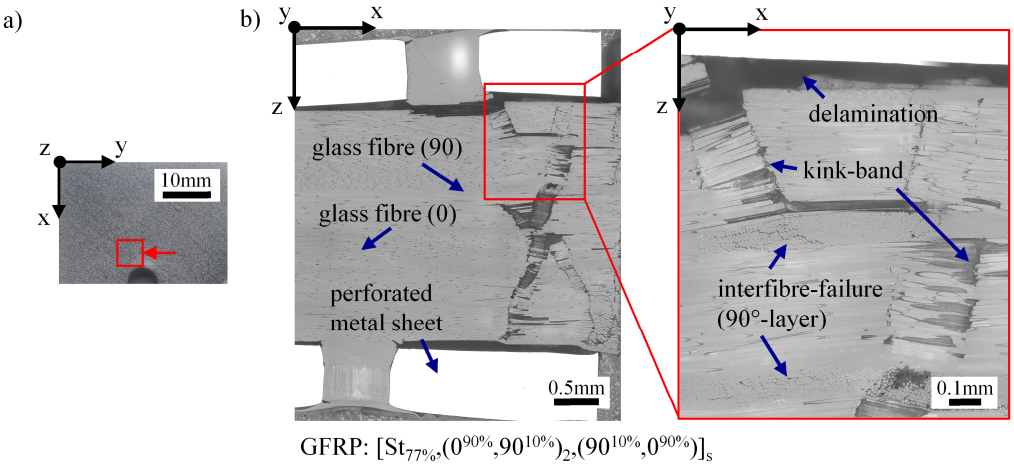

Figure 7. GFRP specimen shortly after 2% hole expansion ($\sigma_{2\%}$~455MPa)
a) sampling of the micrograph specimen, b) optical light microscopy.

Excerpt from ISBN 978-3-00-053387-7

4. Conclusions

In this work the quasi-static bearing response of different FML were characterised and compared with a conventional GFRP laminate. From the results obtained the following conclusions can be drawn. The stainless steel metal sheets demonstrate a high potential in designing high quality FRPs by RTM with enhanced load bearing capability. Furthermore, it allows to keep the thickness of the load introduction area constant which prevents secondary bending of the laminate.

The fibre metal laminates show significant higher bearing strength (up to 33%) and a more ductile fracture behaviour (ε^{br}>700%) in comparison to the GFRP. Without surface treatment, the LM and DIC results show a higher bonding between the perforated metal sheet and the GFRP layer compared to the solid metal sheet/GFRP layer. This prevents significant delamination of the permeable metal sheet and leads to a higher residual strength compared to the hybrid with solid metal sheets. Furthermore, the permeable metal sheet allow the matrix flow through all layers in thickness direction during the VARTM, which increases the process time.

References

[1] Fink A, Camanho PP, Andrés JM, Pfeiffer E, Obst A. Hybrid CFRP/titanium bolted joints: Performance assessment and application to a spacecraft payload adaptor. Composites Science and Technology 2010;70(2):305–17.
[2] Both JC. Tragfähigkeit von CFK-Metall-Laminaten unter mechanischer und thermischer Belastung, Technische Universität München; 2014.
[3] Kolesnikov B, Herbeck L, Fink A. CFRP/titanium hybrid material for improving composite bolted joints. Composite Structures 2008;83(4):368–80.
[4] Vlot A, Gunnink JW. Fibre Metal Laminates. Kluwer Academic Publishers 2001.
[5] Both J, Wedekind M, Baier H. Simulation and experimental characterization of the bearing behavior of CFRP-metal laminates. ECCM15 2012.
[6] Bosbach B, Liebig VW, Fiedler B. Bearing response of fibre metal laminates consisting of GFRP and woven metallic fabrics. ICCM20 2015.
[7] ASTM D5961. Standard Test Method for Bearing Response of Polymer Matrix Composte Laminates. ASTM International 2013.
[8] Irisarri F, Vandellos T, Paulmier P, Laurin F. Experiments and modeling of clamping effects on the the bearing strength of mechanically fastened joint in CFRP laminates. ECCM16 2014.

Excerpt from ISBN 978-3-00-053387-7